

Brain Blood Flow Measured with Intravenous $H_2^{15}O$.

II. Implementation and Validation

M. E. Raichle, W. R. W. Martin, P. Herscovitch, M. A. Mintun, and J. Markham

Washington University School of Medicine, St. Louis, Missouri

We have adapted the well-known tissue autoradiographic technique for the measurement of regional cerebral blood flow (CBF), originally proposed by Kety and his colleagues, for the measurement of CBF in human subjects using positron emission tomography (PET) and intravenously administered oxygen-15-labeled water. This report describes the steps necessary for the implementation of this PET/autoradiographic technique. In order to establish the accuracy of the method, we measured CBF with intravenously administered oxygen-15-labeled water and PET in anesthetized adult baboons and compared the results with blood flow measured by a standard tracer technique that uses residue detection of a bolus of oxygen-15-labeled water injected into the internal carotid artery. The correlation between CBF measured with PET and the true CBF for the same cerebral hemisphere was excellent. Over a blood-flow range of 10–63 ml/(min·100 g), $CBF(PET) = 0.90 CBF(true) + 0.40$ ($n = 23$, $r = 0.96$, $p < 0.001$). When blood flow exceeds 65 ml/(min·100 g) CBF was progressively underestimated due to the known limitation of brain permeability to water.

J Nucl Med 24: 790–798, 1983

In 1951, Kety presented a theory of inert-gas exchange at the lungs and tissues and its possible application to the measurement of tissue blood flow (1). A short time later he and his colleagues described in detail (2,3) a tissue autoradiographic technique for the measurement of local brain blood flow in laboratory animals based on this theory of inert-gas exchange. This autoradiographic technique involved the intravenous infusion of radiolabeled trifluoriodomethane. At the end of 1 min the animal was killed and the brain was removed and sliced in the desired plane for quantitative autoradiography. These quantitative autoradiograms and the time-activity curve of the blood radioactivity formed the basis for the computation of local brain blood flow using Kety's equations (1). This technique has been widely applied and revised on several occasions (4,5) as newer radiotracers were substituted for the volatile and difficult-to-handle trifluoriodomethane.

Because positron emission tomography (PET) provides a quantitative measure of local tissue radioactivity and, hence, an in vivo autoradiogram (6), we reasoned that local cerebral blood flow could be measured in human subjects using the principles of the Kety autoradiographic technique in conjunction with PET and a freely diffusible, inert pharmaceutical labeled with a positron emitter. In Part I (7) we described the theoretical basis for our adaptation of the Kety approach for PET and considered the impact of several potential errors. In this paper we describe the implementation of this technique using $H_2^{15}O$ as the diffusible tracer, and present direct experimental evidence concerning its accuracy.

A preliminary report of this work has been presented (8).

METHODS

Animal preparation. CBF was measured in six adult baboons (*Papio papio*) weighing 18 to 25 kg. To facilitate the injection of small aliquots (approximately 0.2 ml) of the baboon's blood labeled with oxygen-15-water

Received Dec. 21, 1983; revision accepted Apr. 28, 1983.

For reprints contact: M. E. Raichle, MD, Box 8131, Washington University School of Medicine, St. Louis, MO 63110.

into the internal carotid artery, the baboons were anesthetized with phencyclidine (2 mg/kg) at least 2 wk before experiment proper, and the right external carotid artery was ligated at its origin from the common carotid. At the later experiment the radiotracer was injected into the common carotid artery through a small catheter (0.021 cm diam) positioned there under fluoroscopic control.

For the actual comparison of the PET autoradiographic method (7) with the standard residue detection technique using the intracarotid administration of oxygen-15-labeled water (9) the baboons were anesthetized with ketamine (2 mg/kg), paralyzed with gallamine, intubated with a cuffed endotracheal tube, and passively ventilated on a gas mixture containing 70% nitrous oxide and 30% oxygen. The baboons were then positioned on a special couch that permitted placement of the head in the imaging device or over a 3 in. × 2 in. NaI(Tl) scintillation detector appropriately collimated and positioned under the animal's head so as to ensure essentially uniform detection of a single cerebral hemisphere.

To permit the intracarotid injection of oxygen-15-labeled water, a small catheter was inserted percutaneously into the femoral artery and its tip positioned in the right common carotid artery under fluoroscopic control. To prevent clotting in this arterial catheter system, which was used for the injection of the labeled water, monitoring of blood pressure, and sampling of arterial blood, all animals were heparinized at the beginning of the experiment. Arterial pH, P_{CO₂}, and P_{O₂} were measured before and after each injection of tracer. To permit the intravenous injection of oxygen-15-labeled water, a small venous catheter was placed percutaneously in the femoral vein.

Positron emission tomography was performed with the PETT VI system (10), the design and performance characteristics of which have been discussed elsewhere (11,12). Data are recorded simultaneously from seven slices with a center-to-center separation of 14.4 mm. All studies were done in the low-resolution mode, giving an in-plane (i.e., transverse) resolution of 11.7 mm full width at half maximum (FWHM) in the center of the field of view and a slice thickness of 13.9 mm FWHM at the center of the image.

The head of the baboon was positioned with the aid of a vertical laser line such that the center of the lowest slice corresponded to a line running through the center of the cerebral hemispheres. A lateral skull radiograph with this line marked by a vertical radio-opaque wire provided a permanent record of the position of the lowest PET slice. Because of the size of the adult baboon brain (approximately 150 cc) only data from this bottom slice were used in these experiments. Attenuation correction was uniquely determined for each animal by obtaining a transmission scan using a ring source of activity

(germanium-68) fitted to the tomograph as previously described (10).

Single-probe data collection. The signal from the single NaI(Tl) scintillation detector produced by the intracarotid injection of H₂¹⁵O was processed by a pulse-height discriminator with a 60-keV energy window symmetrically bracketing the annihilation peak to minimize scattered radiation. The accepted events (counts) from this single detector were stored in a small laboratory computer. Processing of these data was performed in the computer, including corrections of the count rate for deadtime losses, physical decay of O-15 (T_{1/2} = 123 sec), and background, and conversion to a time-activity plotout. Optimal temporal resolution was achieved in the initial portion of the recording by using sampling integration times of 0.1 sec. Statistically smooth recordings were ensured by injection of sufficient activity into the carotid artery to achieve peak counting rates from 10,000 to 20,000 cps.

PET data collection. For the measurement of CBF with PET a 40-sec emission scan (whose modification to permit longer scan times is discussed below) was performed following an intravenous, bolus injection of 5 ml of saline containing 20–30 mCi of oxygen-15-labeled water. Data collections by PET were started at the time of arrival of radioactivity in the brain as judged by a sudden increase in the bank pair coincidence counting rate of the PETT VI system. This was usually 10–15 sec after tracer injection. Zero time for the study was always the actual time tracer administration commenced. The preparation of the radiowater has been described elsewhere (13). Arterial blood samples were drawn about every 5 sec from the indwelling carotid catheter, starting at the onset of injection and continuing throughout the scan. These samples were weighed and counted in a well counter to obtain O-15 activity as cps/g blood, corrected for physical decay from the time of injection to the time of measurement. The time-activity curve was then constructed.

Calibration of the tomograph to obtain the regional O-15 concentration in the brain from the reconstructed image (cps/cc tissue) was performed by imaging a phantom divided into six wedge-shaped chambers of equal size. The chambers were filled with varying concentrations of carbon-11-labeled bicarbonate. Aliquots from each chamber were counted in the same well counter used for the measurement of blood radioactivity, and the observed counting rate decay-corrected to the start of the phantom scan. From these data (C_{initial}, in cps/cc), the total counts presented to the scanner by 1 cc of target during the length of the scan (C_{total}, in counts/cc) were obtained by integrating the decay curve over the length of the scan T_S:

$$C_{\text{total}} = \int_0^{T_S} C_{\text{initial}} \exp(-kt) dt, \quad (1)$$

where k is the decay constant (per sec) for the tracer. After the phantom image was reconstructed, a regression equation was obtained comparing the relative scan data and the directly measured activity in the phantom. From this relationship, the actual local O-15 concentrations can be obtained from each scan.

Because our scanner does not correct for radioactive decay during the data collection, it is necessary to correct scan data for tracer decay that occurs during the study. Our method is derived by assuming a function of activity that would be constant were it not for decay. This is equivalent to computing the average decay over the scan interval T_S , i.e.,

$$\text{average decay} = \int_0^{T_S} \exp(-kT_S) dt / T_S \quad (2)$$

$$= \frac{1 - \exp(-kT_S)}{kT_S} \quad (3)$$

Inversion of the average decay yields an "average" decay correction. Simulation studies (unpublished) of various functions equivalent to time-varying head-activity curves likely to be encountered during our studies demonstrate that this method of decay correction is quite adequate (i.e., maximum error <4%).

Data analysis. Single detector system. The time-activity curve obtained subsequent to the intracarotid injection of an aliquot of oxygen-15-labeled water was used to compute the mean cerebral transit time for labeled water (t_{H_2O}) (9). The calculation of CBF from t_{H_2O} —which we will call CBF(true) to distinguish it from CBF(PET), the CBF deduced from a PET study—is based on the well-established central volume principle of tracer kinetics (14,15).

The fraction of oxygen-15-labeled water extracted by the brain during a single capillary transit (E) was determined from the same residue curve used for the measurement of CBF(true) following intracarotid injection of $H_2^{15}O$. This single-injection, external-registration technique uses the first 30 sec of the residue curve after the intracarotid injection of labeled water, a method developed in our laboratory for use in vivo with cyclotron-produced positron emitters (9,16,17). With this method E is obtained by graphically extrapolating the relatively slow clearance of the labeled water from brain tissue back to the maximum of the perfusion peak, and computing the ratio

$$E = B/A \quad (4)$$

as shown in Fig. 1. As developed in detail elsewhere by ourselves (17) and others (18–20) the quantity E can be related to the tissue blood flow f [ml/(sec. g)], the capillary surface area (S [cm²/g]) and its permeability (P [cm/sec]) in the following manner:

$$E = 1 - \exp(-PS/f) \quad (5)$$

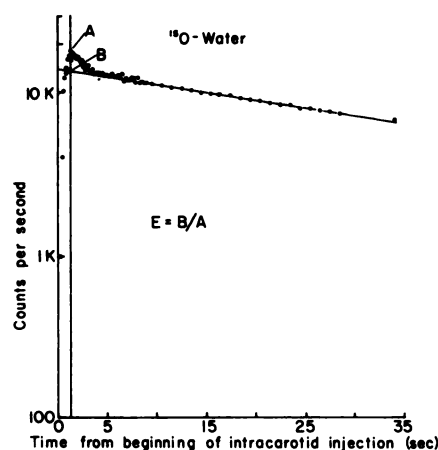


FIG. 1. Brain time-activity curve (semilog) resulting from intracarotid injection of $H_2^{15}O$ in adult baboon. Graphic extrapolation of relatively slow clearance of labeled tissue water back to maximum of perfusion peak allows calculation of fraction of labeled water extracted by tissue (E) during single capillary transit ($E = B/A$). Application of central volume principle of tracer kinetics (see text) to these data allows computation of cerebral blood flow (CBF), which we designate here as CBF(true). Data in this figure were obtained at cerebral blood flow of 102 ml/(min·100 g).

PET system. The blood curve and scan data were analyzed according to the general principles of inert-gas exchange developed by Kety (1) and later embodied in the tissue autoradiographic technique for the measurement of local brain blood flow in laboratory animals (2–5). With this method the local blood flow is obtained by numerically solving the following equation for the constant K

$$C_i(T) = \lambda K \int_0^T C_a(t) \exp[-K(T-t)] dt \\ = \lambda K C_a(T) * \exp(-KT) \quad (6)$$

where $C_i(T)$ is the instantaneous local radiotracer concentration (cps/g) at time, T , derived from a quantitative autoradiogram of a brain slice, and $C_a(t)$ is the measured concentration of radiotracer in arterial blood as a function of time, [cps/ml]; and λ is the brain-to-blood equilibrium partition coefficient for the tracer [ml/g]. λ equals 0.95 in our experiment (9). The operation of convolution is denoted by the asterisk. The constant K is defined by (3):

$$K = mf/\lambda \quad (7)$$

where m is a constant between 0 and 1 that represents the extent to which diffusion equilibrium between blood and tissue is achieved during passage from the arterial to the venous end of the capillary. As further defined by Kety (3)

$$m = 1 - \exp(-PS/f) \quad (8)$$

Thus, m is equivalent to E [Eqs. (7), (8)], a fact that will become important in the analysis of the PET/autoradiographic data (see below).

PET scanners, including the one used in this study (10) do not have adequate temporal resolution to measure tissue radioactivity, $C_i(T)$, instantaneously. Thus, to apply the autoradiographic technique to *in vivo* studies with PET, a scan must run for many seconds, essentially summing the instantaneous radioactivity over time. We have therefore modified the operational equation for this model by an additional integration over the time of the scan (i.e., $T_2 - T_1$) as follows:

$$C = \int_{T_1}^{T_2} C_i(T) dT$$

$$= \lambda K \int_{T_1}^{T_2} C_a(T) * \exp(-KT) dT \quad (9)$$

Here, C is the local number of counts per unit weight of tissue recorded by the tomograph from a region of brain tissue during the scan. The time, T_1 , is chosen as the time at which there is an appreciable increase above background in a selected bank-pair coincidence counting rate of the PETT VI scanner, thus signifying the arrival of radioactivity of the head. In practice, the constant m is assumed to be 1 in the solution of both the tissue [Eq. (6)] and PET [Eq. (9)] operational equations for K . Thus, from Eq. (7), the flow, f , is equal to λK .

This model relates regional CBF to regional tissue counts and the arterial blood radioactivity curve. Unfortunately, the operational Eq. (9) cannot be solved explicitly for blood flow. It can be solved numerically, however, by means of an interactive parameter estimation technique, although this approach requires significant computing time and would be unwieldy given the large number of spatial data to be analyzed. An alternative approach is to use the operational Eq. (9) to generate a lookup table that relates tissue counts to flow for closely spaced values of flow. This involves numerous evaluations of the equation and would require storage and repetitive searching of the table. Instead, we have expressed the operational equation relating blood flow to tissue counts in terms of a second-order polynomial equation:

$$\text{flow} = A (\text{counts})^2 + B (\text{counts}).$$

With this function, a parabola going through the origin, the relationship between flow and counts can be fitted with a less than 0.8% inaccuracy in flow for any given number of counts. In comparison, a first-order linear approximation would introduce errors of up to 5% because the operational equation does deviate somewhat from true linearity (see Fig. 2, Ref. 7). The addition of a second-order polynomial term into the fit thus provides greater accuracy.

CBF was calculated for a single, computer-generated region of interest in the center of the baboon brain. This region of interest was a square with 18 pixels on a side. Because each pixel in the tomographic system is 0.27 cm by 0.27 cm in the horizontal plane and approximately

1.4 cm thick, the volume of brain sampled was $\sim 33 \text{ cm}^3$ or, assuming an average brain density of 1.05 g/cc, 34.7 g. Because the adult baboon brain weighs about 150 g, the volume of tissue we sampled for our data is well below a value that might be in error because of partial-volume effects due to sampling of noncerebral tissue. Placing our region of interest centrally, with equal weight given to both cerebral hemispheres, seemed appropriate despite the fact that our CBF(true) was measured only on the right cerebral hemisphere because no significant asymmetries between hemispheres were noted in our data.

Experimental procedure. CBF was varied in the baboons in two ways. First, the arterial carbon dioxide tension was varied by altering the respiratory rate. At least 20 min were allowed between changes in the respiratory rate to permit a new steady state to be achieved. Measurements of arterial blood gases were obtained before and after all measurements of CBF. In addition to varying the arterial CO_2 tension we used continuous infusions of sodium pentothal (2 g in 500 ml saline) to achieve blood flows less than 20 ml/(min-100 g).

In order to evaluate the effect of PET scan length on the accuracy of the PET/autoradiographic technique we used the list-mode data-gathering capabilities of the system (10), which permitted us to collect data over a period of 120 sec and then reconstruct them into scans of 0-40 sec, 0-80 sec, or 0-120 sec.

Human studies. A single normal adult study* is presented to illustrate the performance of the PET/autoradiographic technique for the measurement of CBF. The subject was prepared for the study by the percutaneous insertion of a small radial-artery catheter under local anesthesia to permit frequent sampling of arterial blood, and the insertion of an intravenous catheter for tracer injection in the opposite arm. The subject's head was positioned in the same manner as that described, above, for the baboons, including alignment with a vertical laser so that the lowest PET slice corresponded to the subject's orbito-meatal line. A lateral skull radiograph (Fig. 2) was obtained with this line marked by a vertical radio-opaque wire to record permanently the orientation of the PET slices in relation to the bony landmarks of the skull. A molded plastic face mask prevented significant head movement during the PET scan. This system, described in detail elsewhere (10), enables accurate repositioning of a subject undergoing sequential studies on different days. After the subject's head was in place in the tomograph, a transmission scan for attenuation correction was performed with a ring phantom containing germanium-68. During the actual measurement of CBF, the room lights were dimmed and the subject instructed to close his eyes. His ears were not plugged. Ambient noise consisted almost entirely of cooling fans from the electronic equipment in the room.

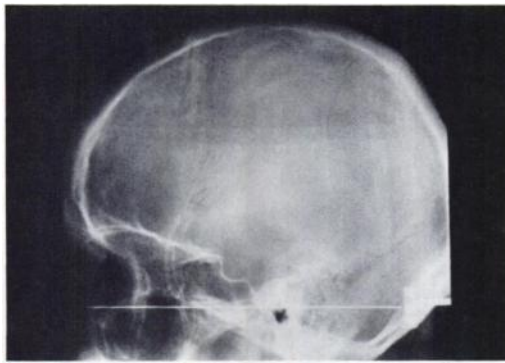


FIG. 2. Lateral skull radiograph of normal, adult human subject showing position (horizontal, radio-opaque line) of lowest of seven PET slices depicted in Fig. 5. Slices are separated by 14 mm (center to center). Radio-opaque wire is 1 mm in diameter.

Because blood samples are drawn from the radial artery in most human subjects (our study follows arteriography, in which case the femoral artery is used) to construct the arterial blood time-activity data for Eq. (10), we anticipated that the intravenously injected radioactivity would arrive at our peripheral sampling site at a time that was different from its arrival time in the brain (usually it arrives later at the peripheral site because of the greater distance from the heart). Because the accuracy of our PET/autoradiographic technique is very sensitive to such differences (7) we correct for them in our human studies by determining the arrival time in the head of the subject by observing and recording the time of an abrupt increase in the coincidence counting rate (sampling from a single bank pair (10) once every second) and the arrival time at the peripheral sampling site from the arterial-blood time-activity curve (see Fig. 5). Differences in the recorded delays are reconciled by shifting the arterial time-activity

curve by the amount of the difference measured in seconds.

RESULTS

Figure 1 presents the first 30 sec of a typical time-activity curve recorded by our single NaI(Tl) scintillation detector collimated to view the injected right cerebral hemisphere of an adult baboon. From the initial portion of this time-activity curve the cerebral hemisphere extraction (E) of oxygen-15-labeled water is calculated according to Eq. (10) and the procedure depicted in the figure. These same data were used to compute CBF(true), the true cerebral blood flow, according to Eq. (6).

The relationship, based on 36 paired measurements, between the CBF(true) and the CBF(PET) is shown in Fig. 3 (left). Between a CBF of 10 and 60 ml/m(min·100 g) the relationship between the two measurements is excellent ($Y = 0.90x + 0.40$; $r = 0.96$), but above a CBF of 60 ml/(min·100 g) the CBF(PET) technique progressively underestimates the CBF(true). Because the intracarotid, residue-detection technique allows us to compute not only the CBF(true) but also the extraction (E) of labeled water [Eq. (4); Fig. 1] for each measurement of CBF(PET) we can evaluate the effect of this diffusion limitation of water on our PET measurement of CBF by dividing each CBF(PET) value by the corresponding value for E. In effect, this corrects for the fact that the value of m [Eq. (9)] is less than the assumed value of 1. The result of this manipulation of the CBF(PET) is shown in Fig. 3 (right). With this correction there occurs excellent agreement between CBF(true) and CBF(PET) over a blood-flow range of 10–155 ml/(min·100 g). Corresponding to this observation is the fact that there is excellent agreement be-

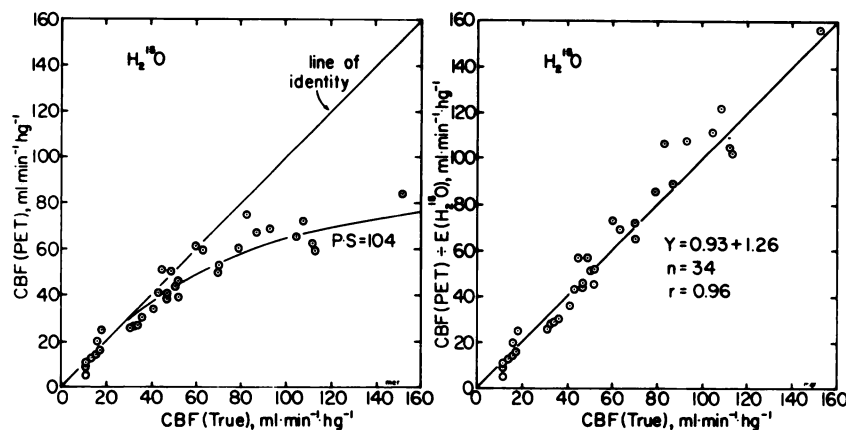


FIG. 3. Comparison between (a) cerebral blood flow measured in adult baboons using PET/autoradiographic technique [CBF(PET)] with intravenous, bolus injection of $H_2^{15}O$, and (b) cerebral blood flow measured in same animal using intracarotid injection of $H_2^{15}O$ and residue detection [CBF(true)]. Data on left represent experimental data. In addition to line of identity, figure contains theoretical line based on computed product of brain permeability times surface area (P·S) for water for these experiments, 104 ml/(min·100 g). This theoretical line is product of CBF(true) and E estimated from Eq. (8) using CBF(true) as F in Eq. (8) along with measured P·S. For tracer with P·S = 104 ml/(min·100 g), CBF(PET) progressively underestimates CBF(true) when latter exceeds 50 ml/(min·100 g). CBF(PET) data on right have been corrected for measured extraction of $H_2^{15}O$ (see text for details).

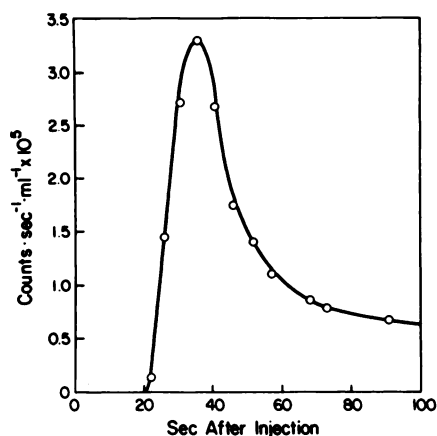


FIG. 4. Typical human arterial-blood, time-activity curve obtained from radial artery following bolus injection of $H_2^{15}O$ in 6 ml of saline into antecubital vein. Note delay in appearance of radioactivity in radial-artery blood (activity injected at time = 0). This delay is compared with delay in arrival of activity in subject's head as signified by abrupt increase in coincidence counts from PETT VI scanner. When differences are observed (radial-artery delay usually exceeds head delay by several seconds) blood curve is shifted to correspond to head delay.

tween the data in Fig. 3 (left) and a line predicted on the basis of the measured P-S for these experiments in the adult baboon [$PS = 104 \pm 11.2$ (s.d.); $n = 25$]. This theoretical line is simply the product of $CBF(\text{true})$ and E estimated from Eq. (8), using $CBF(\text{true})$ as F in Eq. (8) along with the measured P-S for these experiments. Note that P-S could be computed on only 25 of the 36

experiments, because at low CBF where E is unity, P-S is indeterminate.

Varying the length of data collection by PET on the CBF computed by the PET/autoradiographic technique—from the usual 40 sec (i.e., all data in Fig. 2) to 80 or 120 sec—leads to estimates of CBF that decrease as a function of the acquisition time. Thus, in a typical case of CBF decreased from 38 ml/(min·100 g) as measured with the usual 40-sec scan to 32 ml/(min·100 g) with an 80-sec scan and 27 ml/(min·100 g) with a 120-sec scan. A similar decline was observed when the scan length was maintained at 40 sec but the starting time following injection was progressively delayed.

Data from a single, normal, young adult male are shown in Figs. 4 and 5. Typical intravenous injections of 60 to 80 mCi of $H_2^{15}O$ result in bank pair coincidence count rates of 30,000 to 45,000 cps with the PETT VI tomograph in adult subjects. Figure 4 shows the blood time-activity (corrected for decay of O-15) resulting from the intravenous (antecubital) bolus injection of 82 mCi of oxygen-15-labeled water in 6 ml of normal saline. Figure 5 shows data obtained from this study (scan duration = 40 sec).

DISCUSSION

To the best of our knowledge, these data represent the first direct comparison of the classic Kety tissue autoradiographic technique (1-3) with another established technique (i.e., the central volume principle; 14,15) for

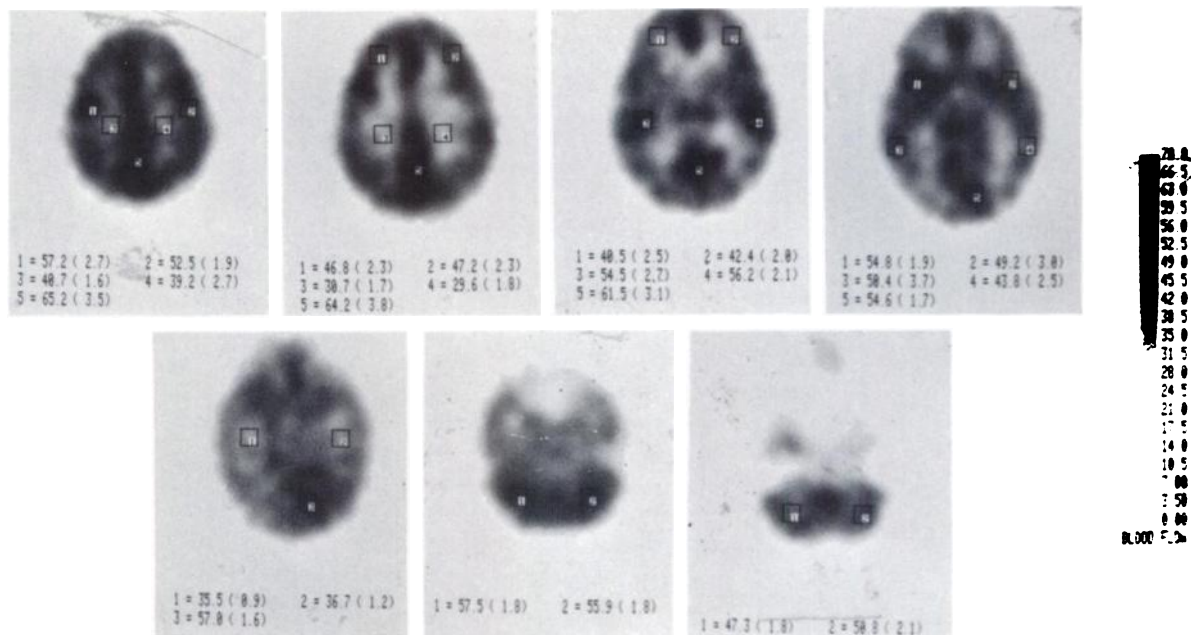


FIG. 5. Typical quantitative measurement of local cerebral blood flow (CBF) in normal, adult, male subject using intravenous bolus injection of 82 mCi of $H_2^{15}O$ and adaptation (7) of classic Kety tissue autoradiographic technique (3). Data were collected over 40 sec. The quantitative gray scale [ml/(min·100 g)] was set to same maximum [i.e., 70 ml/(min·100 g)] for each slice to permit more accurate visual comparison. Specific regions have been selected in each slice (i.e., numbered boxes) to illustrate local variations in blood flow. Values for these regions are listed just below each slice along with standard deviation of 25 pixels in each region.

the measurement of CBF with diffusible, inert indicators. The choice of the latter technique as our standard for comparison seemed especially appropriate to us because it is not affected by the known permeability limitation of the brain for water (9,15). Thus, failure of the PET/autoradiographic technique to estimate accurately the true CBF as the result of a tracer that does not diffuse freely between blood and brain tissue should be easily detectable and quantifiable.

Our data (Fig. 3) clearly indicate that a brain permeability limitation for $H_2^{15}O$ causes an underestimation of CBF, using the PET/autoradiographic technique, when the true brain blood flow exceeds about 60 ml/(min·100 g) in the adult baboon. Values for CBF(PET) above this flow rate are predictably scaled by the extraction of $H_2^{15}O$ [i.e., E, Eq. (4), or m, Eq. (10)] for that blood flow. Three observations support this interpretation of our data. First, division of the CBF(PET) value for blood flow by the extraction of $H_2^{15}O$ for each experiment, measured by the intracarotid injection of $H_2^{15}O$ [Eq. (4); Fig. 1], produces a linear relationship between CBF(true) and CBF(PET) over the entire range of blood flow examined (Fig. 3, right). This manipulation of the experimental data is equivalent to specifying a unique value for m [Eq. (7)], which is normally assumed to have a value of 1 (2,3). Second, the average value for the product (P·S) of brain permeability and surface area, estimated from our data [Eq. (8)] allows us to predict the relationship between the blood flow measured by the PET/autoradiographic technique and the CBF(true). We have illustrated this in Fig. 3 (left) where we have plotted the product of f [i.e., true blood flow per unit weight of tissue, Eq. (6)] and m [Eq. (8)] as a function of CBF(true). It can readily be seen that with a tracer whose apparent P·S product is 104 ml/(min·100 g), CBF is progressively underestimated when blood flow exceeds a value of about 40 ml/(min·100 g). It is also apparent that our experimental data correspond quite well to this hypothetical relationship. Finally, studies of the PET/autoradiographic model using C-11 butanol as the diffusible, inert tracer (to be published separately) demonstrate a linear relationship (i.e., line of identity) between CBF(PET) and CBF(true) [maximum blood flow 120 ml/(min·100 g)]. Because C-11 butanol freely diffuses across the blood-brain barrier (16), this observation further supports our hypothesis that our experimental results reflect the known brain permeability limitation of $H_2^{15}O$.

Other investigators have previously noted that the tissue autoradiographic technique is sensitive to the brain permeability of the diffusible tracer chosen (5,21,22). These observations led to several changes in the choice of tracer for tissue autoradiographic work in small laboratory animals in which CBF can occasionally reach 200–400 ml/(min·100 g).

It is important to understand the clinical implications

of this brain-permeability limitation of $H_2^{15}O$ when it is utilized as the diffusible tracer for the PET/autoradiographic technique. Two facts make us optimistic that $H_2^{15}O$ will perform quite satisfactorily for studies in humans despite its P·S limitation. First, the average brain permeability for water in humans is somewhat higher than we have measured in the baboon in these experiments [i.e., ~104 ml/(min·100 g)]. Paulson and his colleagues report an average P for water in the human brain of 2.4×10^{-4} cm/sec (23). Assuming an average human brain, with capillary surface area of 100 cm²/g (see below), this yields an average P·S (i.e., for gray plus white matter) of 144 ml/(min·100 g) for the human brain. From these data we can estimate that CBF(PET) for the brain as a whole will appreciably underestimate CBF(true) only when the blood flow exceeds ~55 ml/(min·100 g). Second, the above analysis as well as the presentation of our data (Fig. 3) assume a uniform P·S for the brain. Although it is probably reasonable to assume a uniform vascular permeability for the brain, it is not reasonable to assume a uniform capillary surface area when contemplating regional studies in man with PET. In fact, capillary surface area is estimated by others to vary from 190 cm²/cm³ in human cerebral cortex to 57 cm²/cm³ in human cerebral white matter (20,24). Using these data for S one can estimate the true water P·S of gray and white matter from the estimate of human whole-brain P provided by Paulson et al. (i.e., 2.4×10^{-4} cm/sec; Ref. 23). Such an estimate of water P·S for gray and white matter, and the implication it has for the accuracy of the PET/autoradiographic technique are shown in Fig. 6. Based on this information we are quite confident that the PET/autoradiographic technique will perform accurately when applied to regional studies in human subjects (e.g., see Fig. 5). An important test of this assumption will be a direct region-by-region comparison of local CBF measured sequentially with the

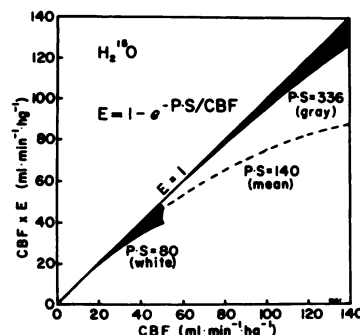


FIG. 6. Hypothetical relationship between cerebral blood flow (CBF) measured with PET/autoradiographic technique in humans (y-axis) and true CBF (x-axis) assuming product of brain white-matter permeability times surface area (P·S) for $H_2^{15}O$ of 80 ml/(min·100 g) and brain gray matter P·S for $H_2^{15}O$ of 336 ml/(min·100 g). These values for P·S of $H_2^{15}O$ are based on whole-brain average for human of 140 ml/(min·100 g) (24). Errors predicted on basis of this analysis are shown as stippled deviations from line of identity.

PET/autoradiographic technique in the same human subject using $H_2^{15}O$ and C-11 butanol. We are currently planning this study.

We emphasize the advantages of $H_2^{15}O$ over alternative inert tracers, labeled with longer-lived radionuclides, that might be selected because of their greater blood-brain barrier permeability (e.g., C-11 butanol, C-11 iodoantipyrine). Because the data collection time for the PET/autoradiographic method must be short (i.e., ≤ 40 sec; see below), approximately equivalent millicurie doses of radiopharmaceutical must be used regardless of the radionuclide. This results in an appreciably higher dose to the subject when longer-lived, positron-emitting radionuclides are used, and more prolonged residual background activity must be tolerated. The consequence of these effects is to reduce greatly the number and frequency of measurements that can be made safely in a single subject. Using $H_2^{15}O$, for example, we have made as many as eight sequential measurements of CBF in a single sitting with the measurements spaced about 12 to 15 min apart. Such a protocol, used in our case for functional mapping of the brain, would be difficult, if not impossible, with tracers labeled with N-13, C-11, or F-18.

There is one very important constraint that must be placed on the use of the PET/autoradiographic technique as well as on the classic tissue autoradiographic technique itself (5). The duration of the study must not exceed 1 min, as originally prescribed by Kety and others (2-5). Data collections in excess of this time period show an underestimation of CBF that increases with time. This phenomenon is also shown in the data of Eklof et al. (21). In the latter study the classic autoradiographic technique was used but direct tissue sampling was substituted for the actual tissue autoradiography. Examining several tracers with differing permeabilities (i.e., antipyrine, ethanol, water, and xenon), Eklof et al. (21) observed a decline in the measured blood flow as the tissue data collection was delayed from 30 sec to 60 or 120 sec. We do not have an explanation for this phenomenon. It is quite clearly not related to any aspect of the PET adaptation of the original Kety autoradiographic technique because it occurs in applications of the original technique (21) as well as in our work. It is definitely not due to the permeability of a particular tracer. We have observed the phenomenon with C-11 butanol as well as $H_2^{15}O$ (unpublished data). Eklof et al. (21) have observed it with an additional group of tracers with widely differing permeabilities. It is not due to tissue inhomogeneity, as Eklof et al. (21) discuss in detail. Until this problem has been solved, investigators must be cautioned to use this technique—whether in the original form or in the PET adaptation—with strict attention to the length of data collection. This *must not exceed* 1 min for accurate, quantitative results.

One practical feature of the PET/autoradiographic

technique should be emphasized. Because the tissue concentration of radionuclide is related to local blood flow in a nearly linear manner (7), a PET *image* of the distribution of $H_2^{15}O$ or other suitable radiopharmaceutical (e.g., C-11 butanol) is an accurate representation of local tissue blood flow. Where regional comparisons in the same brain provide the desired clinical information, sampling of arterial blood may be unnecessary. In addition, accumulating data in humans (to be published separately) indicate that comparisons between sequential scans in the same person can be made when the scans are scaled to the exact amount of $H_2^{15}O$ injected and careful attention is paid to the positioning of the subject in the PET scanner.

Finally, when sampling of arterial blood from a radial artery is necessary for a truly quantitative measurement of CBF using the PET/autoradiographic technique, we stress that this can be accomplished with relative safety and minimal discomfort to the human subject. The risk to the subject is minimized by performing an Allen test (25) to document a dual arterial supply to the hand; and using a 20-gauge or smaller Teflon catheter for relatively short periods of time (26). At the time of this writing, we have performed approximately 360 such catheterizations without a complication. Our experience agrees with the much greater experience of others that suggests a complication rate (i.e. major ischemic complication) of less than one in 1000 (27-29).

FOOTNOTE

* Permission for this study was obtained from the subject in accordance with guidelines approved for this study by the Human Studies Committee of Washington University and the Radioactive Drug Research Committee (Washington University) of the Food and Drug Administration.

ACKNOWLEDGMENT

This research was supported by NIH grants NS06833, NS14834, HL13851, RR00396, and RR01380. Drs. Herscovitch and Martin were Fellows of the Medical Research Council of Canada.

REFERENCES

1. KETY SS: The theory and application of the exchange of inert gas at the lungs and tissues. *Pharmacol Rev* 3:1-41, 1951
2. LANDAU WM, FREYGANG WH JR, ROWLAND LP, et al: The local circulation of the living brain; values in the unanesthetized and anesthetized cat. *Trans Am Neurol Assoc* 80:125-129, 1955
3. KETY SS: Measurement of local blood flow by the exchange of an inert, diffusible substance. *Methods Med Res* 8:228-236, 1960
4. REIVICH M, JEHLE J, SOKOLOFF L, et al: Measurement of regional cerebral blood flow with antipyrine- ^{14}C in awake cats. *J Appl Physiol* 27:296-300, 1969
5. SAKURADA O, KENNEDY C, JEHLE J, et al: Measurement of local cerebral blood flow with iodo[^{14}C]antipyrine. *Am J Physiol* 234:H59-H66, 1978
6. RAICHEL ME: Quantitative in vivo autoradiography with positron emission tomography. *Brain Res Rev* 1:47-68, 1979

7. HERSCOVITCH P, MARKHAM J, RAICHLER ME: Brain blood flow measured with intravenous $H_2^{15}O$. I. Theory and error analysis. *J Nucl Med* 24:782-789, 1983
8. HERSCOVITCH P, MARKHAM J, RAICHLER ME: Accuracy of the Kety autoradiographic measurement of cerebral blood flow adapted for positron emission tomography. *J Nucl Med* 23:P13, 1982 (abstr)
9. EICHLING JO, RAICHLER ME, GRUBB RL JR, et al: Evidence of the limitation of water as a freely diffusible tracer in brain of the Rhesus monkey. *Circ Res* 35:358-364, 1971
10. TER-POGOSSIAN MM, FICKE DC, HOOD JT SR, et al: PETT VI: A positron emission tomograph utilizing cesium fluoride scintillation detectors. *J Comput Assist Tomogr* 6: 125-133, 1982
11. FICKE DC, BEECHER DE, HOFFMAN GR, et al: Engineering aspects of PETT VI. *IEEE Trans Nucl Sci* 29: 474-478, 1982
12. YAMAMOTO M, FICKE DC, TER-POGOSSIAN MM: Performance study of PETT VI, a positron computed tomograph with 288 cesium fluoride detectors. *IEEE Trans Nucl Sci* 29:529-533, 1982
13. WELCH MJ, LIFTON JT, TER-POGOSSIAN MM: Preparation of millicurie quantities of oxygen-15-labeled water. *J Labelled Compd* 5:168-172, 1969
14. ZIERLER KL: Equations for measuring blood flow by external monitoring of radioisotopes. *Circ Res* 16:309-321, 1965
15. ROBERTS GW, LARSON KB, SPAETH PE: The interpretation of mean transit time measurements for multiphase systems. *J Theor Biol* 39:447-475, 1973
16. RAICHLER ME, EICHLING JO, STRAATMANN MG, et al: Blood-brain barrier permeability of ^{11}C -labeled alcohols and ^{15}O -labeled water. *Am J Physiol* 230:543-552, 1976
17. RAICHLER ME, LARSON KB: The significance of the $NH_3-NH_4^+$ equilibrium on the passage of ^{13}N -ammonia from blood to brain. A new regional residue detection model. *Circ Res* 48:913-937, 1981
18. SANGREN WC, SHEPPARD CW: A mathematical derivation of the exchange of a labeled substance between a liquid flowing in a vessel and an external compartment. *Bull Math Biophys* 15:387-394, 1953
19. RENKIN EM: Transport of potassium-42 from blood to tissue in isolated mammalian skeletal muscles. *Am J Physiol* 197: 1205-1210, 1959
20. CRONE C: The permeability of capillaries in various organs as determined by use of the "indicator diffusion" method. *Acta Physiol Scand* 58:292-305, 1963
21. EKLÖF B, LASSEN NA, NILSSON L, et al: Regional cerebral blood flow in the rat measured by the tissue sampling technique; a critical evaluation using four indicators C^{14} -antipyrine, C^{14} -ethanol, H^3 -water and xenon 133 . *Acta Physiol Scand* 91:1-10, 1974
22. ECKMAN WW, PHAIR RD, FENSTERMACHER JD, et al: Permeability limitation in estimation of local brain blood flow with [^{14}C]antipyrine. *Am J Physiol* 229:215-221, 1975
23. PAULSON OB, HERTZ MM, BOLWIG TG, et al: Filtration and diffusion of water across the blood-brain barrier in man. *Microvasc Res* 13:113-124, 1977
24. COBB S: Cerebrospinal blood vessels. In *Penfield's Cytology and Cellular Pathology of the Nervous System*. New York, Hoeber, 1932, Vol II, pp 577-610
25. OH TE, DAVIS NJ: Radial artery cannulation. *Anaesth Intens Care* 3:12-18, 1975
26. DAVIS FM: Radial artery cannulation: influence of catheter size and material on arterial occlusion. *Anaesth Intens Care* 6:49-53, 1978
27. DALTON B, LAVER MB: Vasospasm with an indwelling radial artery cannula. *Anesthesiology* 34:194-197, 1971
28. BEDFORD RF, WOLLMAN H: Complications of percutaneous radial-artery cannulation: an objective prospective study in man. *Anesthesiology* 38:228-236, 1973
29. DAVIS FM, STEWART JM: Radial artery cannulation: a prospective study in patients undergoing cardiothoracic surgery. *Br J Anaesth* 52:41-47, 1980

**The Society of Nuclear Medicine Computer & Instrumentation Councils
The Technology of NMR
A Symposium for Scientists and Physicians**

February 5-6, 1984

Call for Papers

Orlando, Florida

The Society of Nuclear Medicine Computer & Instrumentation Councils will present "The Technology of NMR," a symposium for scientists and physicians, February 5-6, 1984 in Orlando, Florida.

You are invited to submit papers which address the technological problems associated with this new modality. Of specific interest are design of and requirements for NMR instrumentation, imaging techniques for spatial encoding, problems of pulse sequencing, image processing and display, as well as spectroscopy. Development of methodology and phantom design for applications to system evaluation are also of interest.

Submit a 200 word abstract and four copies to:

Dr. R.E. Johnson
Department of Radiology
Imaging Division
The School of Medicine
University of North Carolina
Chapel Hill, North Carolina 27514

Authors will be required to submit a camera-ready manuscript at the meeting for publication in the proceedings.

Abstracts must be received by October 1, 1983.